Research Article Vol. 61, No. 26 / 10 September 2022 / Applied Optics 7565

applied optics

Optimization of the nonlinear crystal length for high-power single-frequency intracavity frequency-doubling lasers

Yongrui Guo,[1,2] Jing Su,[1,3] and Huadong Lu[1,3,*]

[1]State Key Laboratory of Quantum Optics and Quantum Optics Devices, Institute of Opto-Electronics, Shanxi University, Taiyuan, Shanxi 030006, China
[2]School of Optoelectronic Engineering, Chongqing University of Posts and Telecommunications, Chongqing 400065, China
[3]Collaborative Innovation Center of Extreme Optics, Shanxi University, Taiyuan, Shanxi 030006, China
*Corresponding author: luhuadong@sxu.edu.cn

Received 13 July 2022; revised 20 August 2022; accepted 20 August 2022; posted 22 August 2022; published 6 September 2022

We report a method of optimizing the nonlinear crystal length of the intracavity frequency-doubling laser, which is achieved by maximizing the output power of the frequency-doubling laser in the case of ensuring the single longitudinal mode (SLM) operation of the laser. The optimal length of the nonlinear crystal for an SLM oscillation of the intracavity frequency-doubling laser is firstly theoretically predicted by comparing the losses introduced by the nonlinear crystal with different lengths with that of ensuring the SLM operation of the laser. Then three nonlinear LiB_3O_5 (LBO) crystals with the length of 18, 20, and 22 mm are adopted to be the frequency-doubling components in the experiment. By recording the output power and monitoring the longitudinal mode structure of the laser, it is found that the nonlinear LBO crystal with the length of 20 mm is the best candidate, since the output power is higher than that of the LBO crystal with the length of 18 mm, and the SLM operation of the laser is readily achieved compared to that of the LBO crystal with the length of 22 mm. The experimental results well agree with the theoretical predictions. The current method can pave a good way to attain a single-frequency continuous-wave intracavity frequency-doubling laser. © 2022 Optica Publishing Group

https://doi.org/10.1364/AO.470487

1. INTRODUCTION

The single-frequency continuous-wave (CW) solid-state green laser source has important applications in a broad range of scientific applications, including quantum optics, high-resolution spectroscopy, atomic physics, precision measurements [1–6], and so on, owing to their intrinsic advantages of good beam quality, high stability, and narrow linewidth as well as low noise. In order to achieve a stable single-frequency CW green laser with high output power, intracavity frequency doubling is an effective candidate because of its high intracavity power density [7,8]. However, with the increase of the output power of the single-frequency CW green laser, in addition to the severe thermal effects of the optical elements [9,10], the longitudinal mode stability becomes also fragile due to the drastic intracavity mode competition of the fundamental wave (FW) laser. In this case, different longitudinal modes can couple each other through the nonlinear crystal, and "green problem" can occur [11,12]. The frequent mode hopping and multilongitudinal-mode (MLM) oscillation directly increases the intensity and frequency noises of the laser [13,14]. Therefore, it is important to simultaneously achieve high output power and optical conversion efficiency as well as stable single longitudinal mode (SLM) operation for a single-frequency CW intracavity frequency-doubling laser. In 2005, Greenstein and Rosenbluh analyzed the influence of the nonlinear spectral bandwidth on the longitudinal mode structure (LMS) of a single-frequency and intracavity frequency-doubling laser [15]. They proved that the laser can work with SLM operation only if the ratio γ between the nonlinear spectral bandwidth of the nonlinear crystal and the gain bandwidth of laser crystal was larger than a certain value. They also showed that using a short nonlinear crystal and narrowing the gain bandwidth can maximize the γ value. In 2007, an etalon was used to act as a spectral filter and then actively inserted into the intracavity frequency-doubling laser to reduce the gain bandwidth of laser crystal [16]. As a result, a long-term stable single-frequency intracavity frequency-doubling laser has been successfully realized. However, the loss introduced by the etalon greatly restricted the output power of the laser. In addition, if we want to adopt a short nonlinear crystal to obtain a stable single-frequency and intracavity frequency-doubling laser, the output power of the second-harmonic-wave (SHW) laser and conversion efficiency of the laser will be influenced because both of them are directly proportional to the

square of nonlinear crystal length. It means that it is of particular importance to find a new way to optimize the length of the nonlinear crystal to attain a stable single-frequency and frequency-doubling laser with high output power and optical conversion efficiency. In this paper, based on the SLM condition of a laser, we report a new method to optimize the nonlinear crystal length of a single-frequency and frequency-doubling laser. We theoretically and experimentally demonstrate that the optimal nonlinear crystal length should be close to the critical value where the normalized nonlinear loss introduced by second-harmonic generation (SHG) of the intracavity frequency-doubling laser equals that for SLM operation of the laser.

2. THEORETICAL ANALYSIS

According to the physical condition of SLM operation for high-power solid-state lasers [17], the relationship between the normalized intracavity nonlinear loss ε_0 and the normalized linear loss α_0 for single-frequency intracavity frequency-doubling lasers should satisfy the following inequality:

$$\varepsilon_0 > \frac{-(2\beta+1)\alpha_0^2}{4\beta^2\alpha_0 + 2\beta\alpha_0 - 4\beta^2}. \tag{1}$$

When ε_0 is larger than the right side of Eq. (1), the laser can operate with SLM; otherwise, MLM and mode-hopping phenomena will occur [17]. In Eq. (1), the normalized linear loss can be given by $\alpha_0 = \frac{\delta+t}{2g_0 l}$, where δ is the intracavity linear loss and t is the transmissivity of the output coupler at FW, $g_0 l = K P_{\text{in}}$, where K and P_{in} are the factor of the pump and the pump power, respectively. For intracavity frequency-doubling lasers pumped with the pump power P_{in}, the pump factor K of the laser can be obtained according to the method demonstrated in Ref. [18]. In addition, the output coupling mirror of the lasers is usually coated with high-reflection film at the FW so as to increase the intracavity FW power density and scale up the optical power of the lasers. Therefore, the normalized linear loss α_0 of the lasers can be seen as a certain value for the lasers with the fixed laser resonator and pump power. On the right side of Eq. (1), β can be described as

$$\beta = \frac{1}{2} - 2\text{sinc}^2\left(\frac{1.39}{2\gamma}\right), \tag{2}$$

where γ is defined as the ratio between the nonlinear spectral acceptance bandwidth ($\Delta\lambda_n$) of the nonlinear crystal and the gain bandwidth ($\Delta\lambda_g$) of the laser crystal. The gain bandwidth $\Delta\lambda_g$ is also a certain value while the material of the gain medium is determined. The nonlinear spectral acceptance bandwidth $\Delta\lambda_n$ can be given by

$$\Delta\lambda_n = \frac{\text{const}}{l_{nc}}, \tag{3}$$

where the constant in Eq. (3) depends on the properties of the nonlinear crystal, the phase-matching method, as well as the laser wavelength at the FW. Therefore, γ can be written as

$$\gamma = \frac{\text{const}}{\Delta\lambda_g l_{nc}}. \tag{4}$$

From Eq. (4), we can see that γ is only inversely proportional to the nonlinear crystal length l_{nc} when the materials of the nonlinear crystal and the gain medium are both determined.

The normalized nonlinear loss ε_1 introduced by the SHG of the intracavity frequency-doubling laser is defined as the ratio of the nonlinear loss to the round-trip unsaturated gain for a fundamental power density at which the saturated laser gain is just equal to one-half its unsaturated value [12], which can be given by

$$\varepsilon_1 = \frac{\eta S_0}{4g_0 l}, \tag{5}$$

where S_0 is the saturation intensity, which is described as $S_0 = h\nu/\sigma\tau$, h is the Planck constant, ν is the laser frequency, σ is the stimulated emission cross section, and τ is the lifetime of the laser energy level. Under the condition that the frequency-doubling crystal works at the optimal phasing-matching temperature, the nonlinear conversion factor η can be given by

$$\eta = \frac{8\pi^2 d_{\text{eff}}^2 l_{nc}^2 \omega_l^2}{\epsilon c \lambda_f^2 n^3 \omega_{sh}^2}, \tag{6}$$

where d_{eff} is the effective nonlinear coefficient, ϵ is the vacuum permittivity, c is the velocity of light, n is the refractivity of the nonlinear crystal, λ_f is the wavelength of the laser at FW, and ω_l and ω_{sh} are the beam waists at the place of the laser medium and the nonlinear crystal, respectively.

From Eqs. (5) and (6), we can clearly see that ε_1 is proportional to the square of the nonlinear crystal length l_{nc}. However, according to Eqs. (1)–(4), we can also find that a longer nonlinear crystal length will in turn result in a small value of γ, which can influence ε_0 and impact the LMS of the laser. For simultaneously realizing the high output power and single-frequency operation of intracavity frequency-doubling lasers, the values of ε_1 and ε_0 of the lasers with different nonlinear crystal lengths l_{nc} must be qualitatively compared. Therefore, the relationship between ε_1 and l_{nc}, and the relationships between ε_0, l_{nc}, and α_0 were numerically simulated by taking the laser parameters in Table 1 into Eqs. (1) and (5). In Table 1, the intracavity linear loss δ of the laser is 4.1%, which was obtained by employing the method demonstrated in Ref. [18]. The numerical results are shown in Fig. 1, wherein pictures of (a), (b), (c), and (d) corresponded to the laser with the LiB_3O_5 (LBO) crystal length of 18, 20, 21.83, and 24 mm, respectively. In panels (a)–(d) of Fig. 1, the red line, the black circle, and the blue triangle were the critical curve for MLM and SLM oscillation of the laser, ε_0 with respect to $\alpha_0 = 3.23 \times 10^{-3}$, and ε_1 introduced by the SHG of the laser, respectively, at the pumping power of $P_{\text{in}} = 80$ W. From panels (a)–(d) of Fig. 1, we can see that by increasing l_{nc} from 18, 20, and 21.83 mm to 24 mm, ε_0 rapidly increased from 4.39×10^{-7}, 9.68×10^{-6}, and 5.87×10^{-5} to 1.01×10^{-2}, while ε_1 slowly increased from 3.99×10^{-5}, 4.93×10^{-5}, and 5.87×10^{-5} to 7.10×10^{-5}. For $l_{nc} < 21.83$ mm, ε_1 was always larger than ε_0 for the same l_{nc}, which meant that the intracavity frequency-doubling laser can operate in the SLM region. In this region, increasing the nonlinear crystal length close to $l_{nc} = 21.83$ mm can scale up the output power of the SHW laser. For $l_{nc} \approx 21.83$ mm, $\varepsilon_0 \approx \varepsilon_1$; in this case, the LMS of the laser will be switching between SLM and MLM oscillation

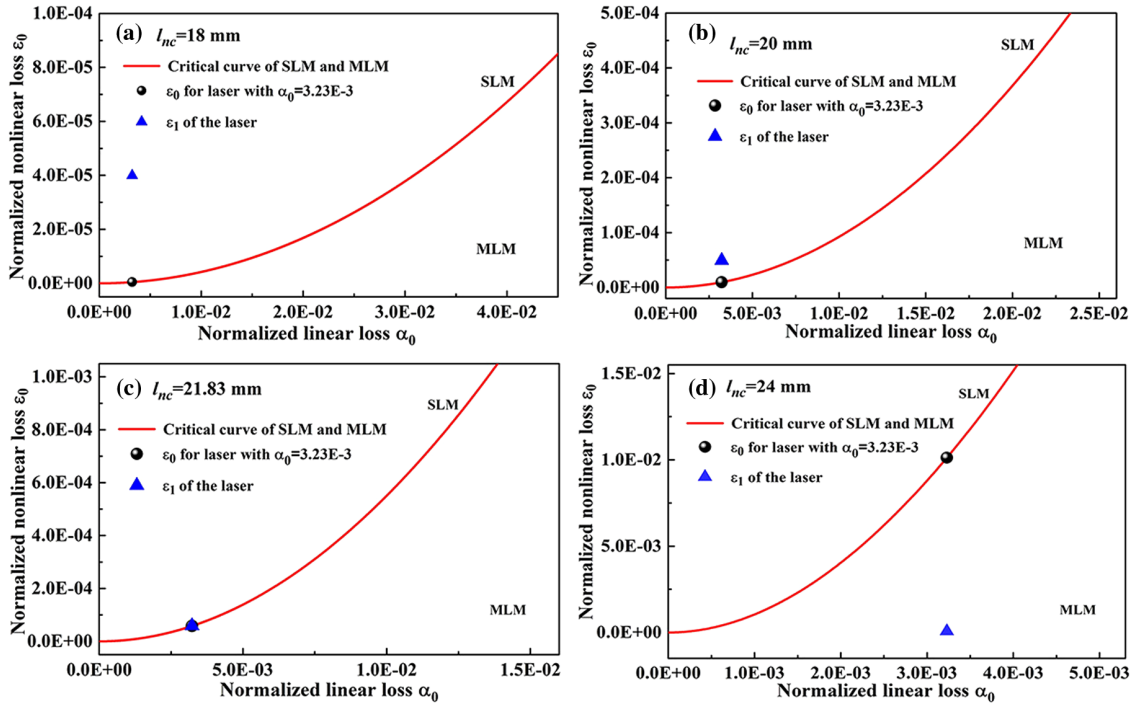

Fig. 1. Numerical simulations of the relationship between ε_0, l_{nc}, and α_0 of the laser, and the relationship between ε_1 and l_{nc} of the laser. Panels (a), (b), (c), and (d) correspond to the lasers with $l_{nc} = 18$ mm, 20 mm, 21.83 mm, and 24 mm, respectively. The red line, the black circle, and the blue triangle in the panels are with respect to the critical curve of SLM and MLM oscillation, ε_0 with respect to $\alpha_0 = 3.23 \times 10^{-3}$, and ε_1 for the laser with l_{nc}, respectively.

along with mode-hopping phenomena. For $l_{nc} > 21.83$ mm, ε_1 introduced by SHG cannot afford to ε_1 required for SLM oscillation of the laser, and MLM oscillation of the laser will be taking place. The theoretical critical value of 21.83 mm for simultaneously achieving SLM operation and high output power of the SHW laser is also less than that of 24 mm calculated from the Rayleigh length equation of $2 * Z_R = \frac{2*\pi\omega_{sh}}{\lambda_f}$ upon considering the beam divergence. Therefore, the critical nonlinear crystal length for SLM operation of the intracavity frequency-doubling laser can be theoretically delimited when the incident pump power and the intracavity linear loss of the laser are determined. Moreover, the optimal nonlinear crystal length for simultaneously achieving SLM operation and high output power of intracavity frequency-doubling lasers can also be obtained, which should be close to the theoretical critical value.

Table 1. Parameters of the Intracavity Frequency-Doubling Laser by Employing the Type-I Noncritically Phase-Matched Lithium Triborate (LBO) Crystal

const	2263 GHz*mm
$\Delta\lambda_g$	255 GHz
δ	4.1%
S_0	8.30827×10^6 W/mm^2
K	0.09 W^{-1}
P_{in}	80 W
d_{eff}	1.16×10^{-12} V/m
ε	8.85×10^{-12} F/m
c	3×10^8 m/s
n	1.56
λ_f	1064 nm
ω_l	420 μm
ω_{sh}	62 μm
t	0.5%

3. EXPERIMENTAL SETUP

The theoretical analysis for the method of optimizing nonlinear crystal length to simultaneously achieve the single-frequency operation and high output power intracavity frequency-doubling laser was experimentally verified. The diagram of the experiment setup is shown in Fig. 2. The pumping source was a fiber coupled laser diode with the center wavelength of 888 nm and a maximum output power of 80 W. The diameter and the numerical aperture of the coupling fiber were 400 μm and 0.22, respectively. The pump radiation was focused into the gain medium by two coupling lenses with the focal lengths of 30 and 80 mm, respectively. A figure-eight-shaped ring resonator constructed by four mirrors ($M_1 - M_4$) was designed. M_1 and M_2 were two concave–convex mirrors with a curvature radius of 1500 mm. The input coupler M_1 was coated with high transmissivity (HT) films at 888 nm ($T_{888\,\text{nm}} > 95\%$) and high-reflection (HR) films at 1064 nm ($R_{1064\,\text{nm}} > 99.5\%$). M_2 and M_3 were coated with HR films ($R_{1064\,\text{nm}} > 99.5\%$) at 1064 nm. M_3 and M_4 were two plane-concave mirrors with a curvature radius of 100 mm. The output coupler M_4 was coated with HR films at 1064 nm ($R_{1064\,\text{nm}} > 99.5\%$) and HT films at 532 nm ($T_{532\,\text{nm}} > 95\%$). The gain medium was an a-cut composite

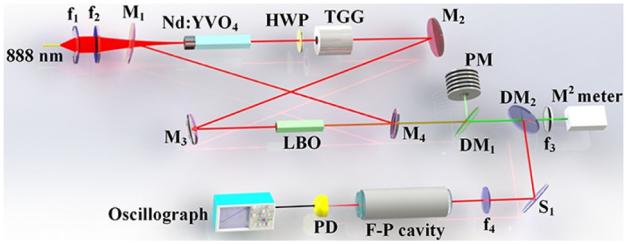

Fig. 2. Schematic diagram of the experimental setup. TGG, terbium gallium garnet; HWP, half-wave plate; LBO, lithium triborate; DM_1, DM_2, dichroic mirrors; PM, power meter; PD, photodiode detector.

YVO_4/Nd : YVO_4 rod with an undoped end cap of 3 mm and a 0.8 at.% Nd-doped part of 20 mm. At the second end face of the gain medium, there existed a wedge angle of 1.5 deg for achieving the stable polarization of the laser [19]. The front end face of the Nd : YVO_4 crystal was coated with antireflection (AR) films at 1064 and 888 nm ($R_{1064\,nm;888\,nm} < 0.25\%$), and the second end face was coated with AR films at 1064 nm ($R_{1064\,nm} < 0.25\%$). To eliminate the spatial hole burning effect and realize the unidirectional operation of the laser, an optical diode comprising an 8 mm long terbium gallium garnet (TGG) crystal and a half-wave plate (HWP) was employed. The type-I non-critically phase-matched LBO crystal (S_1, S_2: $AR_{1064\,nm;532\,nm}$) with the cross section of $3 \times 3\ mm^2$ was employed as the nonlinear crystal due to its large temperature acceptance bandwidth combined with a high optical damage threshold. For achieve a high frequency-doubling efficiency, the LBO crystal was placed at the beam waist between M_3 and M_4, and whose temperature was controlled at the optimal phase matching of 149.0°C with a precision of 0.01°C. The output laser beams at 1064 and 532 nm were separated by the dichroic mirror, and the output power of the 532 nm laser was monitored by the power meter (LabMax-Top, Coherent). The LMS of the 532 nm laser was monitored by scanning the confocal Fabry–Perot (F-P) cavity with a free spectral range of 750 MHz and finesse of 120, respectively.

4. EXPERIMENTAL RESULTS

When the temperatures of the LBO crystals were set to the optimal phase-matching temperature of 149.0°C, the output powers of the 532 nm laser with the increase of the incident pump power were first recorded for LBO crystals with the lengths of $l_{nc} = 18$ mm, $l_{nc} = 20$ mm, and $l_{nc} = 22$ mm and shown as the (a) black curve, (b) blue curve, and (c) red curve in Fig. 3, respectively. From Fig. 3, it can be seen that the output power of the 532 nm laser was 18.56 ± 0.19 W for the LBO crystal with the length of $l_{nc} = 18$ mm. When it was replaced by the LBO crystals with the lengths of $l_{nc} = 20$ mm and $l_{nc} = 22$ mm, the output powers of single-frequency 532 nm lasers were increased to 20.54 ± 0.21 W and 21.60 ± 0.22 W, respectively. Especially, once the incident pump power was beyond 70 W, the rising trend was obviously enhanced with the increase of the LBO crystal length, which benefited from the large nonlinear conversion efficiency owing to the length increase of the LBO crystal. The theoretical predictions for LBO crystals with different lengths under the incident pump power of

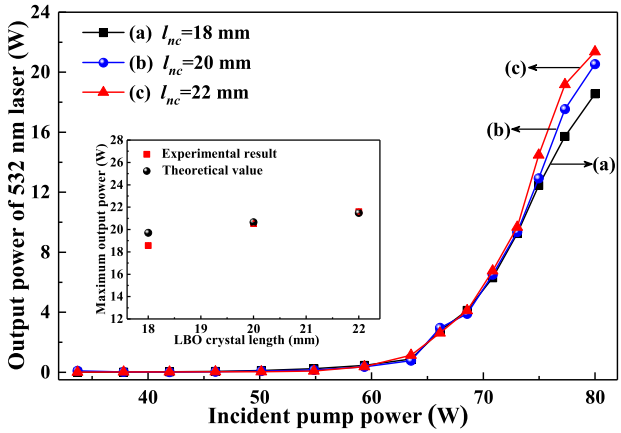

Fig. 3. Output powers of 532 nm lasers with the LBO crystal lengths of (a) $l_{nc} = 18$ mm, (b) $l_{nc} = 20$ mm, and (c) $l_{nc} = 22$ mm versus the incident pump power. The inset shows the experimentally measured and theoretically calculated corresponding maximum output powers of the 532 nm lasers.

80 W was also implemented and compared to the experimental results, which are depicted in the inset of Fig. 3. It can be known that the experimental measured maximum output powers of 18.56 ± 0.19 W, 20.54 ± 0.21 W, and 21.60 ± 0.22 W for LBO crystals with the lengths of $l_{nc} = 18$ mm, $l_{nc} = 20$ mm, and $l_{nc} = 22$ mm are consistent with the numerical simulation results of 19.70, 20.65, and 21.49 W for the laser, respectively.

The monitored LMSs of the CW single-frequency and intracavity frequency-doubling 532 nm laser by using the F-P interferometer were recorded and illustrated in Fig. 4 while the LBO crystals with different lengths were being employed in the experiment. Though the output power of the single-frequency 532 nm laser was lower for the LBO crystals with length of 18 mm and 20 mm than that of the 22 mm length of the LBO crystal, it was easy to attain stable SLM operation for the laser, as shown in Fig. 4(a). On the contrary, the output power of the single-frequency 532 nm laser was highest for the LBO crystal with the length of 22 mm, but it was very difficult to achieve the stable SLM operation. In the process of the observation, the side modes can often appear and oscillate together with the main longitudinal mode, as shown in Fig. 4(b). From the output power and the LMS of the laser, it was clear that although a long nonlinear LBO crystal increased the nonlinear conversion efficiency and output power of the single-frequency 532 nm laser, it also narrowed the nonlinear spectral acceptance bandwidth, which resulted in narrowing the stability range of the SLM operation of the laser. By comparison, it was obvious that employing the LBO crystal with the length of 20 mm was more beneficial for simultaneously achieving the high output power and stable SLM oscillation of the laser. The experimental results agreed well with the numerical simulations, which indicated the validity of the presented method for optimizing nonlinear crystal length to realize the high-power and single-frequency operation of the intracavity frequency-doubling laser. The power stability of the single-frequency intracavity frequency-doubling laser with LBO crystal length of $l_{nc} = 20$ mm was measured and is depicted in Fig. 5. At the output power of 20.56 ± 0.21 W, the peak-to-peak power stability of the laser for 6 h was measured to

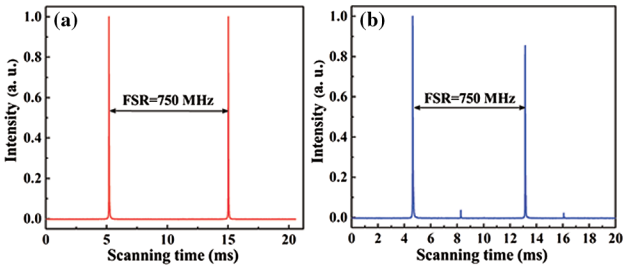

Fig. 4. Measured LMSs of intracavity frequency-doubling lasers with (a) $l_{nc} = 18$ mm and $l_{nc} = 20$ mm, and (b) $l_{nc} = 22$ mm.

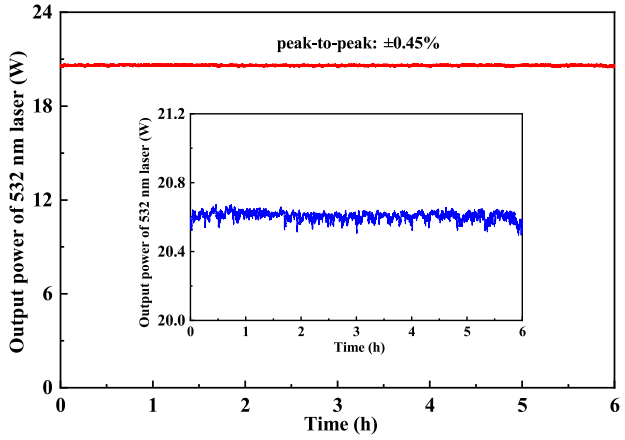

Fig. 5. Long-term power stability of 532 nm laser for 6 h.

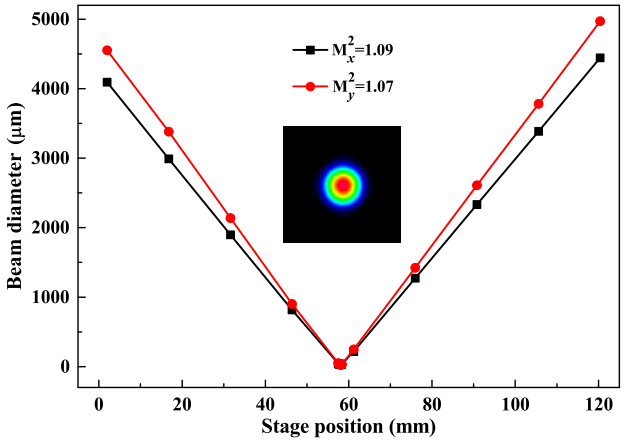

Fig. 6. Measured beam quality of 532 nm laser.

be better than ±0.45%, illustrating that the laser can be stable oscillating with SLM without the need for active stabilization. The beam quality of the laser was measured by an M2 meter (M2SETVIS, Thorlabs); the measured values of M_2^x and M_2^y were 1.09 and 1.07, respectively. The measured caustic curve and the corresponding spatial beam profile are shown in Fig. 6 and its inset, respectively.

5. CONCLUSION

In summary, we have proposed and executed a method of optimizing the length of the nonlinear crystal to achieve a single-frequency and intracavity frequency-doubling laser with high output power. We theoretically predicted the optimal nonlinear crystal of a single-frequency and intracavity frequency-doubling laser by comparing the nonlinear loss introduced by the nonlinear crystal to that of achieving the SLM operation. According to the theoretical prediction, the optimal length of the LBO crystal was 21.83 mm for the incident pump power of 80 W. The corresponding critical nonlinear loss was 3.23×10^{-3}. Then, in the experiment, by utilizing the LBO crystals with the lengths of 18, 20, and 22 mm, respectively, as the frequency-doubling components of a single-frequency laser, the output power and the LMS were explored and compared. It was verified that the highest output power was attained by employing the LBO crystal with the length of 20 mm in the case of ensuring the stable SLM operation of the laser, compared to 18 and 22 mm LBO crystals. The experimental results agreed well with the theoretical predictions. We believe that this paper can provide an effective way to optimize the nonlinear crystal length, which is very important for achieving high-power and single-frequency intracavity frequency-doubling lasers.

Funding. National Natural Science Foundation of China (61975100, 62027821, 62105192); Basic Research Project of Shanxi Province (201901D211186, 20210302121004); Program for the Innovative Talents of High Education Institution of Shanxi; Fund for Shanxi '1331 Project' Key Subjects Construction; Chongqing University of Posts and Telecommunications (A2022-288).

Disclosures. The authors declare no conflicts of interest.

Data availability. Data underlying the results presented in this paper are not publicly available at this time but may be obtained from the authors upon reasonable request.

REFERENCES

1. E. J. Zang, J. P. Cao, Y. Li, C. Y. Li, Y. K. Deng, and C. Q. Gao, "Realization of four-pass I_2 absorption cell in 532-nm optical frequency standard," IEEE Trans. Instrum. Meas. **56**, 673–676 (2007).
2. J. R. Abo-Shaeer, C. Raman, J. M. Vogels, and W. Ketterle, "Observation of vortex lattices in Bose-Einstein condensates," Science **292**, 476–479 (2001).
3. X. C. Yao, H. Z. Chen, Y. P. Wu, X. P. Liu, X. Q. Wang, X. Jiang, Y. Deng, Y. A. Chen, and J. W. Pan, "Observation of coupled vortex lattices in a mass-imbalance Bose and Fermi superfluid mixture," Phys. Rev. Lett. **117**, 145301 (2016).
4. J. Simon, W. S. Bakr, R. Ma, M. E. Tai, P. M. Preiss, and M. Greiner, "Quantum simulation of antiferromagnetic spin chains in an optical lattice," Nature **472**, 307–312 (2011).
5. J. R. Gair, I. Mandel, A. Sesana, and A. Vecchio, "Probing seed black holes using future gravitational-wave detectors," Class. Quantum Grav. **26**, 125–134 (2009).
6. H. Z. Chen, X. P. Liu, X. Q. Wang, Y. P. Wu, and Y. X. Wang, "30 W, sub-kHz frequency-locked laser at 532 nm," Opt. Express **26**, 33756–33763 (2018).
7. Y. J. Wang, Y. H. Zheng, C. D. Xie, and K. C. Peng, "High-power low-noise Nd: YAP/LBO laser with dual wavelength outputs," IEEE J. Quantum Electron. **47**, 1006–1013 (2011).
8. Q. W. Yin, H. D. Lu, and K. C. Peng, "Investigation of the thermal lens effect of the TGG crystal in high-power frequency-doubled laser with single frequency operation," Opt. Express **23**, 4981–4990 (2015).
9. Y. J. Wang, Y. H. Zheng, Z. Shi, and K. C. Peng, "High-power single-frequency Nd:YVO_4 green laser by self-compensation of astigmatisms," Laser Phys. Lett. **9**, 506–510 (2012).

10. Q. W. Yin, H. D. Lu, J. Su, and K. C. Peng, "High power single-frequency and frequency-doubled laser with active compensation for the thermal lens effect of terbium gallium garnet crystal," Opt. Lett. **41**, 2033–2036 (2016).
11. K. I. Martin, W. A. Clarkson, and D. C. Hanna, "Self-suppression of axial mode hopping by intracavity second-harmonic generation," Opt. Lett. **22**, 375–377 (1997).
12. R. G. Smith, "Theory of intracavity optical second-harmonic generation," IEEE J. Quantum Electron. **6**, 215–223 (1970).
13. T. Baer, "Large-amplitude fluctuations due to longitudinal mode coupling in diode-pumped intracavity-doubled Nd:YAG lasers," J. Opt. Soc. Am. B **3**, 1175–1180 (1986).
14. Y. Guo, H. Lu, M. Xu, J. Su, and K. Peng, "Investigation about the influence of longitudinal-mode structure of the laser on the relative intensity noise properties," Opt. Express **26**, 21108–21118 (2018).
15. S. Greenstein and M. Rosenbluh, "The influence of nonlinear spectral bandwidth on single longitudinal mode intra-cavity second harmonic generation," Opt. Commun. **248**, 241–248 (2005).
16. Y. H. Zheng, H. D. Lu, F. Q. Li, K. S. Zhang, and K. C. Peng, "Four watt long-term stable intracavity frequency-doubling Nd:YVO_4 laser of single-frequency operation pumped by a fiber-coupled laser diode," Appl. Opt. **46**, 5336–5339 (2007).
17. H. D. Lu, J. Su, Y. H. Zheng, and K. C. Peng, "Physical conditions of single-longitudinal-mode operation for high-power all-solid-state lasers," Opt. Lett. **39**, 1117–1120 (2014).
18. Y. R. Guo, H. D. Lu, Q. W. Yin, and J. Su, "Intra-cavity round-trip loss measurement of all-solid-state single-frequency laser by introducing extra nonlinear loss," Chin. Opt. Lett. **15**, 021402 (2017).
19. Y. H. Zheng, F. Q. Li, Y. J. Wang, K. S. Zhang, and K. C. Peng, "High-stability single-frequency green laser with a wedge Nd:YVO_4 as a polarizing beam splitter," Opt. Commun. **283**, 309–312 (2010).